Contributions to Tobacco & Nicotine Research
formerly: Beiträge zur Tabakforschung International
Volume 33 · No. 3 · June 2024
DOI: 10.2478/cttr-2024-0006

Design of Draw Resistance of Pressure Drop Standards for Tobacco Products Based on the Flow Distribution *

by

Pengfei Zhang [1], Congcong Li [2], Rongchao Yang [1], Zhandong Shi [1], Zhihao Chen [1], Kai Zhang [2], and Qian Miao [1]

[1] *Zhengzhou Tobacco Research Institute of CNTC, Zhengzhou 450001, China*
[2] *China Jiliang University, Hangzhou 310018, China*

SUMMARY

Cigarette draw resistance and filter pressure drop are both critical physical indicators for the tobacco industry, which use testing equipment to measure the two parameters. Pressure drop standards are used as transfer standards to ensure the accuracy and reliability of the testing equipment. Pressure drop standards are generally cylindrical rods having a certain number of parallel capillaries. To address the issue of how to design and fabricate pressure drop standards quickly and conveniently, this paper proposes a design method for pressure drop standards based on structural parameters. The method uses a mathematical model of the internal airflow of the standard including the entrance effect into a circular capillary and uses an iterative calculation algorithm accordingly. By iterative calculation, the structural parameters of the pressure drop standard, namely, diameter and length of the capillaries, were obtained, along with the relationship between the draw resistance of the standard and the flow rate in each capillary. The accuracy of the mathematical model was validated by comparing and analyzing the experimental and theoretical draw resistance of standards with different structural parameters. The experimental results showed that the relative error between the measured draw resistance and the calculated draw resistance was below 8%, which proves the reliability and validity of the mathematical model, and provides theoretical support for the design and fabrication of pressure drop standards. [Contrib. Tob. Nicotine Res. 33 (2024) 164–172]

KEYWORDS

Structural parameters; pressure drop standard; design; capillaries size; length.

ZUSAMMENFASSUNG

Zigarettenzugwiderstand und Filterdruckabfall sind beides kritische physikalische Indikatoren für die Tabakindustrie, die zur Messung dieser beiden Parameter Prüfgeräte einsetzt. Druckabfallstandards werden als Transferstandards verwendet, um die Genauigkeit und Zuverlässigkeit der Prüfgeräte zu gewährleisten. Druckabfallstandards bestehen im Allgemeinen aus einer bestimmten Anzahl paralleler Kapillaren. Besonders wichtig ist die Frage, wie

*Received: 18th August 2023 – accepted: 24th April 2024

This work is licensed under a Creative Commons Attribution-NonCommercial-ShareAlike 4.0 International License (CC BY-NC-SA 4.0).
Authors who publish with this journal retain all copyrights and agree to the terms of the above-mentioned CC BY-NC-SA 4.0 license.

man ein geeignetes Normal herstellt. Um die Frage zu klären, wie Druckabfallstandards schnell und bequem entworfen und hergestellt werden können, wird in diesem Beitrag eine Methode für Druckabfallstandards auf der Grundlage von Strukturparametern vorgeschlagen. Die Methode hat ein mathematisches Modell der internen Luftströmung des Standards auf der Grundlage des Eintrittseffekts eines kreisförmigen Rohrs aufgestellt und einen entsprechenden iterativen Berechnungsalgorithmus entwickelt. Durch iterative Berechnung wurden die strukturellen Parameter des Druckabfallstandards, nämlich der Kapillarendurchmesser und die Länge des Kapillarrohrs, sowie die Beziehung zwischen dem Zugwiderstand des Normals und der Durchflussmenge jedes Kapillarrohrs, ermittelt. Die Genauigkeit des mathematischen Modells wurde durch den Vergleich und die Analyse des experimentellen und theoretischen Zugwiderstands von Standards mit verschiedenen strukturellen Parametern validiert. Die experimentellen Ergebnisse zeigten, dass der relative Fehler zwischen dem gemessenen und dem berechneten Zugwiderstandswert innerhalb von 8% lag, was die Zuverlässigkeit und Gültigkeit des mathematischen Modells der internen Luftströmung im Standard zeigt und eine theoretische Unterstützung für die Konstruktion und Herstellung von Druckabfallstandards bietet. [Contrib. Tob. Nicotine Res. 33 (2024) 164–172]

RESUME

La résistance à l'aspiration de la cigarette et la perte de charge du filtre sont deux indicateurs physiques essentiels pour l'industrie du tabac, qui utilise des équipements de test pour mesurer ces deux paramètres. Les étalons de perte de charge sont utilisés comme étalons de transfert pour garantir la précision et la fiabilité de l'équipement de test. Les étalons de perte de charge sont généralement composés d'un certain nombre de capillaries parallèles. Il est particulièrement important de savoir comment fabriquer un étalon approprié. Pour répondre à la question de savoir comment concevoir et fabriquer rapidement et commodément des étalons de perte de charge, cet article propose une méthode de conception des étalons de perte de charge basée sur des paramètres structurels. La méthode établit un modèle mathématique du flux d'air interne de la norme basé sur l'effet d'entrée d'un tuyau circulaire et développe un algorithme de calcul itératif en conséquence. Le calcul itératif permet d'obtenir les paramètres structurels de l'étalon de perte de charge, à savoir la taille des capillaries et la longueur du tube capillaire, ainsi que la relation entre la résistance à l'aspiration de l'étalon et le débit de chaque tube capillaire. La précision du modèle mathématique est validée par la comparaison et l'analyse de la résistance à l'étirement expérimentale et théorique des étalons avec différents paramètres structurels. Les résultats expérimentaux montrent que l'erreur relative entre la valeur mesurée de la résistance à l'étirement et la valeur calculée de la résistance à l'étirement est inférieure à 8%, ce qui prouve la fiabilité et la validité du modèle mathématique de l'écoulement interne de l'air dans l'étalon et apporte un soutien théorique à la conception et à la fabrication d'étalons à chute de pression. [Contrib. Tob. Nicotine Res. 33 (2024) 164–172]

INTRODUCTION

Cigarette draw resistance and filter pressure drop are both major physical parameters that affect the composition of cigarette smoke and sensory quality (1). The tobacco industry measures draw resistance of cigarettes and filter pressure drop by means of specific testing equipment, which is calibrated with pressure drop transfer standards. The ISO 6565 standard (2) specifies the basic characteristics of the pressure drop standards and calibration methods. Currently, there exist many studies on the calibration method and environmental conditions of the pressure drop standard. The tobacco industry carries out metrological calibration of the pressure drop standard based on ISO 6565. YANG *et al.* (3) proposed a method to improve the accuracy of the calibration results by using the volume flow rate regulation method, and compared it with the standard critical flow orifice (CFO) method to analyze the differences in repeatability and stability between the two methods when calibrating the pressure drop standard. FAN *et al.* (4) conducted draw resistance testing experiments at different atmospheric pressures in Zhengzhou, Guiyang, and Kunming, and analyzed the relationship between draw resistance and atmospheric pressure, and proposed a correction method for draw resistance measurement results at high altitudes. KEITH and CORBIN (5) described a simple device, consisting of a collection of glass capillary tubes, which can be used as a stable, pressure insensitive standard for calibrating pressure drop machines. COLARD *et al.* (6) pointed out that environmental parameters have an influence on the airflow characteristics of the standard in realistic situations, and established a correction model for the multi-capillary pressure drop standard.

Most of the current research focuses on the calibration method of the pressure drop standard and the effect of environmental conditions on the pressure drop standard, but there are no reports on methods for quantitative calculation of the internal air flow in the pressure drop standard. Based on the structural parameters of a pressure drop standard containing ten parallel capillaries, a flow model was established including the effects of the laminar flow in the inlet section and the flow distribution in the capillaries.

This model allowed calculating the draw resistance of the pressure drop standard, which can provide theoretical guidance for the design of the pressure drop standard.

MATERIALS AND METHODS

Materials and equipment

Materials: Seven pressure drop standards with specifications of around 1–8 kPa, numbered 1–7, and conditioned according to ISO 4302 (7) for 48 hours.

Equipment: Digital pressure gauge Fluke RPM4 (Fluke, Everett, WA, USA); Critical Flow Orifice (CFO) standard (Cerulean, Milton Keynes, UK); Optical gaging products (OGP) vision measurement system (Hexagon, Stockholm, Sweden) with a resolution of 1 µm.

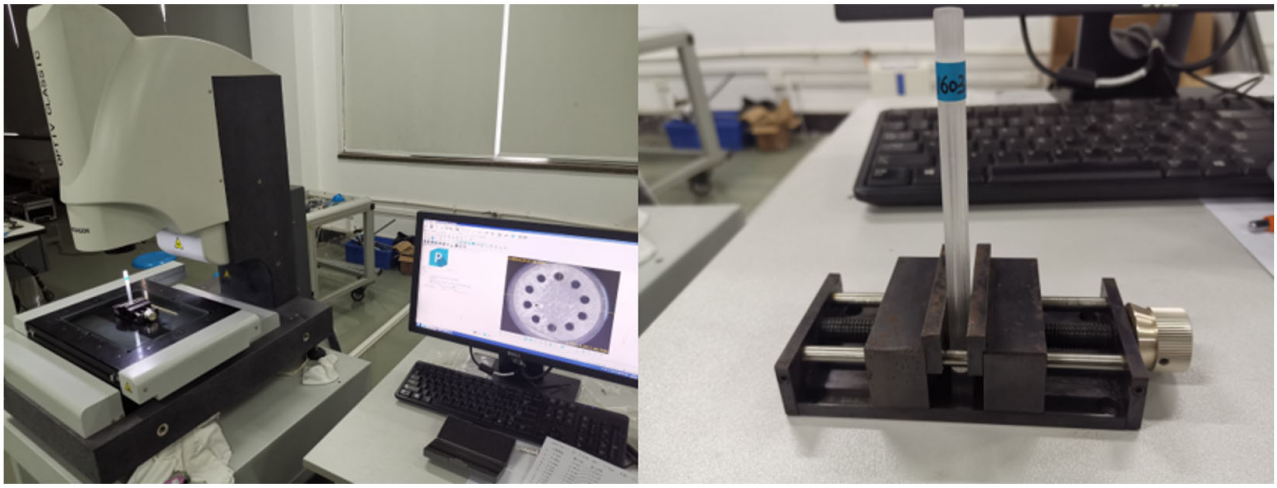

Figure 1. Optical gaging product (OGP) test instrumentarium.

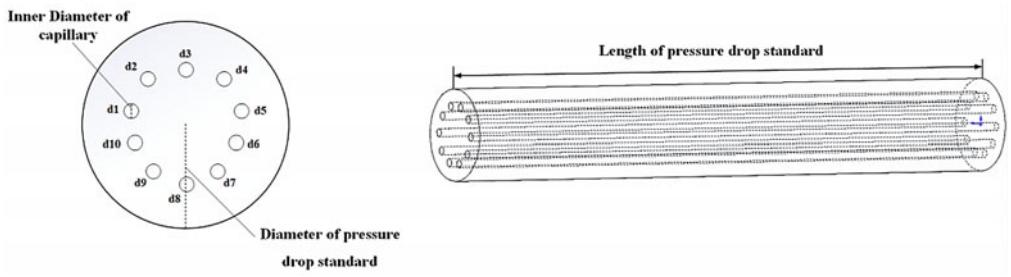

Figure 2. Geometric structure and schematic diagram of pressure drop standards.

Method

The structural parameters, including capillary diameter and overall length of pressure drop standards were measured using an OGP image measurement device. The pressure drop standard was fixed using a clamping device so that the cross-section of the standard was parallel to the bottom surface of the test bench. OGP's camera focused on the end face of the standard. The experimental instrumentation is shown in Figure 1.

Commencing from a reference point, the diameters of the ten capillaries were measured in clockwise manner and denoted as d1 to d10 successively. The left panel of Figure 2 illustrates a schematic representation of the end face of the pressure drop standard, while the right panel shows a length diagram of the pressure drop standard. The pressure drop standard was placed horizontally on the test stand and the test software was opened. After that, one end of the standard was searched to draw a boundary line. The camera movement was used to find the other end of the rod to perform the same operation. The software was used to determine the distance between the two lines, i.e. the length of the standard. During empirical testing, we observed that the data from both ends of the pressure drop standard exhibited minimal variance. Consequently, we selected the geometric data from one end for documentation in Table 1. Standard constant flow orifice (CFO) calibration of the pressure drop standard is illustrated in Figure 3. The gas flow rate at the output end of the pressure drop standard controlled by the standard constant flow orifice should be 17.50 ± 0.30 mL/s. Initially, the gas supply switch was turned on, all flow resistances were removed to zero the pressure difference gauge, and the digital differential pressure gauge was zeroed. Then, the pressure drop standard was placed in a dedicated fixture, the air valve was opened, and the pressure difference between the two ends of the rod was tested using a digital differential pressure gauge. Recordings were taken at 2-min intervals,

Table 1. Geometric parameters of pressure drop standard.

Parameter	Capillary no. (mm)									
	d1	d2	d3	d4	d5	d6	d7	d8	d9	d10
Inner diameter of capillary	0.643	0.635	0.634	0.635	0.630	0.630	0.622	0.637	0.640	0.635
Diameter of pressure drop standard	7.981									
Length of pressure drop standard	120.432									

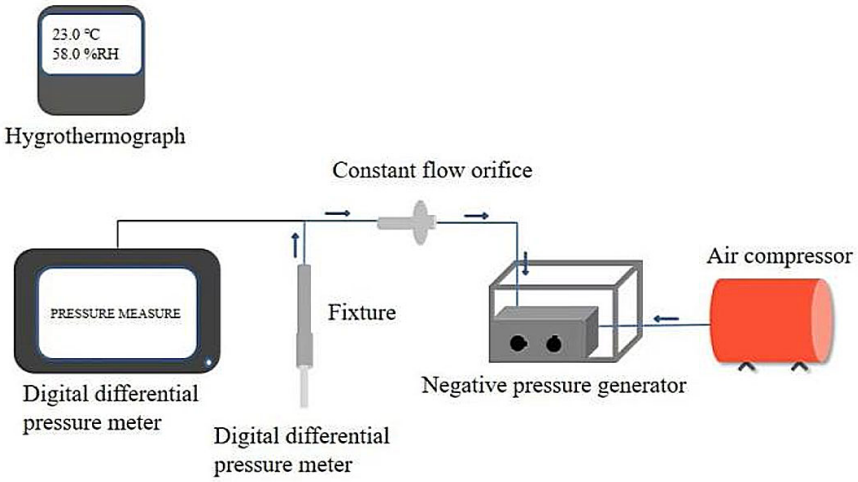

Figure 3. Schematic diagram of pressure drop standard calibration device based on the critical flow orifice (CFO) method.

capturing data five times until a state of stability was reached, indicated by no further changes in the reading after 10 min. This final reading represented the draw resistance of the pressure drop standard.

The measurement process was repeated three times, and the average reading obtained at the 10-min mark served as the calibrated value for the pressure drop standard. The calibration results were reported with a precision of 0.1 Pa.

Theoretical analysis

The flow of the gas passing through a capillary of the pressure drop standard can be regarded as laminar flow in a circular capillary. After the gas flows into the capillary at a uniform velocity u_m, a boundary layer will be generated near the wall under the action of viscosity. The mass flow through the capillary is constant, and the thickness of the boundary layer increases gradually along the capillary. The velocity of the part that is not affected by the boundary layer will increase until the boundary layer intersects at the center of the capillary cross section, which is the length of the developing section. The flow of the gas after the developing section develops fully. Thus, the total length of the pressure drop standard can be divided into two parts: the developing section L_D and the fully developed section $L_{developed}$. The flow distribution in a capillary of the pressure drop standard is shown in Figure 4, where P_0 is the inlet pressure and $\delta(x)$ is the thickness of the boundary layer.

We have conducted a detailed simulation analysis of the inlet and outlet sections of the capillary, taking into account the disturbances and turbulences that may be caused by sudden contraction or expansion during testing. The simulation results are shown in Figure 5, where Figure 5 (a) displays the velocity cloud diagram of the inlet section, and Figure 5 (b) displays that of the outlet section. It is clear from the figure that there is a fully developed cross-section at the air inlet. In contrast, the turbulence effect at the outlet is not significant. Therefore, in subsequent discussions, we did not consider the turbulence effect at the outlet.

The pressure drop along a rough capillary in steady flow of an incompressible viscous fluid is related to the length of the capillary L, the capillary diameter d, the absolute roughness ε, the average velocity u_m, and the fluid density ρ. Based on the fundamental principles of fluid mechanics, the pressure drop can be expressed as:

$$\Delta P = f(\mathrm{Re}, \frac{\varepsilon}{d}) \frac{L}{d} \frac{\rho u_m^2}{2} \quad [1]$$

Let $\lambda = f$ (Re, ε/d), which is called the energy loss coefficient, the value of which is determined by experiment, then the equation [1] can be expressed as:

$$\Delta P = \lambda \frac{L}{d} \frac{\rho u_m^2}{2} \quad [2]$$

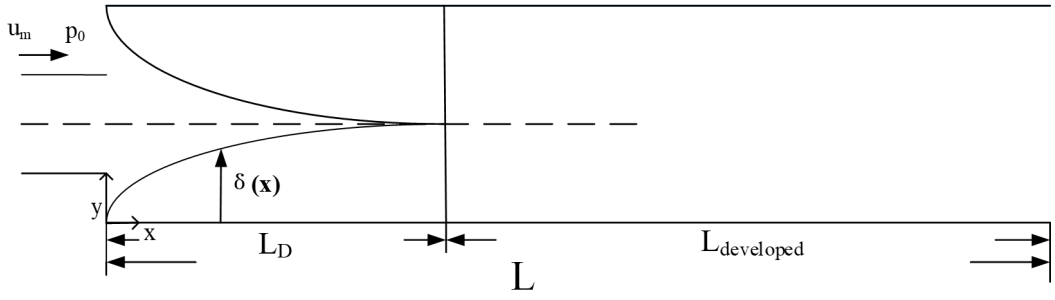

Figure 4. Schematic diagram of the developing and fully developed flow sections in a capillary of the pressure drop standard.

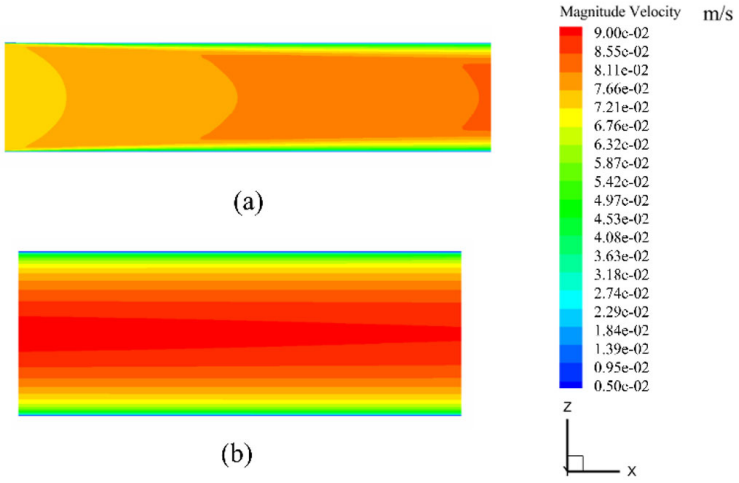

Figure 5. Velocity cloud diagrams of the inlet and outlet sections.

Equation [2] is applicable to both laminar and turbulent flows. The volumetric flow rate Q is:

$$Q = u_m \cdot A \quad [3]$$

where A is the cross-sectional area of the capillary, then equation [2] can be expressed as:

$$\Delta P = \lambda \frac{L}{d} \frac{\rho}{2A^2} Q^2 \quad [4]$$

The total flow resistance R is defined as:

$$R = \lambda \frac{L}{d} \frac{\rho}{2A^2} \quad [5]$$

So:

$$\Delta P = R \cdot Q^2 \quad [6]$$

The total flow resistance R is divided into the developing section and fully developed section and can be expressed as:

$$R = R_D + R_{developed} \quad [7]$$

where R_D represents the flow resistance of the developing section, and $R_{developed}$ represents the flow resistance of the fully developed section.

Derivation of the flow resistance in the developing section

According to WANG (8), on the inlet section of circular capillary for laminar and turbulent flows, the length of the developing section can be obtained as:

$$L_D = 0.0288 \,\mathrm{Re} \cdot d \quad [8]$$

where Re is the Reynolds number of the flow, d is the diameter of the capillary.

The pressure loss coefficient λ_p in the developing section can be expressed as:

$$\lambda_p = \frac{P_0 - P}{\frac{1}{2}\rho u_m^2} = \frac{\Delta P}{\frac{1}{2}\rho u_m^2} \quad [9]$$

where P_0 is the inlet pressure, P is the pressure at a certain position, ρ is the gas density, and u_m is the gas velocity. Comparing with equation [2], the pressure drop in the developing section can be expressed as:

$$\Delta P_1 = \lambda_p \cdot \frac{1}{2}\rho u_m^2 = \lambda \frac{L}{d} \cdot \frac{1}{2}\rho u_m^2 \quad [10]$$

As shown in Figure 6, the pressure drop from the inlet section to the i-th section in the developing section, which is divided into n segments, can be expressed as:

$$\Delta P_i = \lambda_{pi} \cdot \frac{1}{2}\rho u_m^2 = \sum_{j=1}^{n} \lambda_j \frac{L_j - L_{j-1}}{d} \cdot \frac{1}{2}\rho u_m^2 = \sum_{j=1}^{n} \lambda_j \frac{\Delta L_j}{d} \cdot \frac{1}{2}\rho u_m^2 \quad [11]$$

The relationship between the pressure loss coefficient λ_{pi} from the inlet to the i-th segment and the pressure loss coefficient λ_i of the i-th segment can be expressed as:

$$\lambda_{pi} = \sum_{j=1}^{n} \lambda_j \frac{\Delta L_j}{d} \quad [12]$$

where λ_p can be obtained by looking up the corresponding table in (8). When the thickness of the boundary layer reaches its maximum, i.e., the junction between the developing section and the fully developed section, we have:

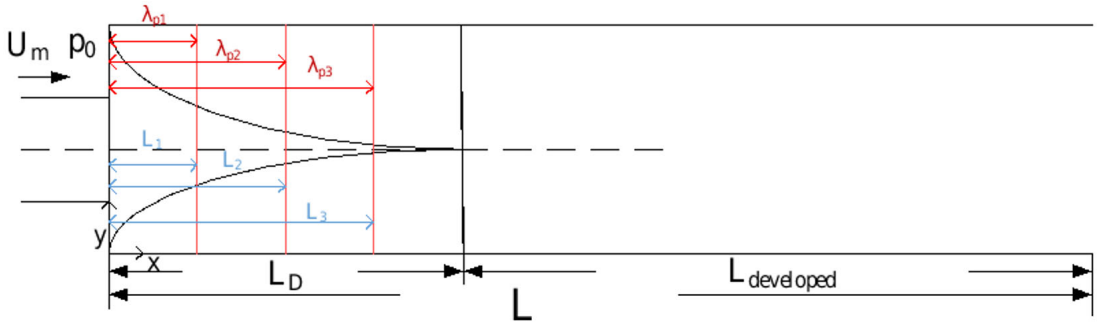

Figure 6. Schematic diagram of segmentation in the developing section.

$$\lambda_p = \sum_{i=1}^{n} \lambda_i \frac{\Delta L_i}{d} = 4 \qquad [13]$$

Combined with equation [7], the flow resistance of the developing section can be expressed as:

$$R_D = \left(\sum_{i=1}^{n} \lambda_i \frac{\Delta L_i}{d} \right) \frac{\rho}{2A^2} = 4 \frac{\rho}{2A^2} \qquad [14]$$

Derivation of flow resistance in the fully developed section

The flow in the developed section is laminar. According to NIKURADSE (9), in laminar flow, the friction coefficient varies only with the Reynolds number, regardless of relative roughness, and the method for calculating the friction coefficient along the length of the capillary is:

$$\lambda_{developed} = \frac{64}{\mathrm{Re}} \qquad [15]$$

Combined with the calculated length L_D in equation [8], the flow resistance of the fully developed section can be expressed as:

$$R_{developed} = \frac{\lambda_{developed}}{d} \left(L - L_D \right) \frac{\rho}{2A^2} \qquad (16)$$

where L represents the total length of the pressure drop standard.

Calculation of flow distribution for the pressure drop standard

Based on the above analysis, an iterative calculation algorithm was established, as shown in Figure 7. In accordance with the previously mentioned resistance theory, given the pressure drop value, we could verify the value by calculating with the theoretical capillary diameter. To validate the accuracy of the theory, seven pressure drop standards were created. An iterative approach was used to guide the allowable deviation in the theoretical diameter of the pressure drop standards and to instruct the deviation of the pressure drop standards based on the range of diameter variations. Given that the total flow rate was constant and

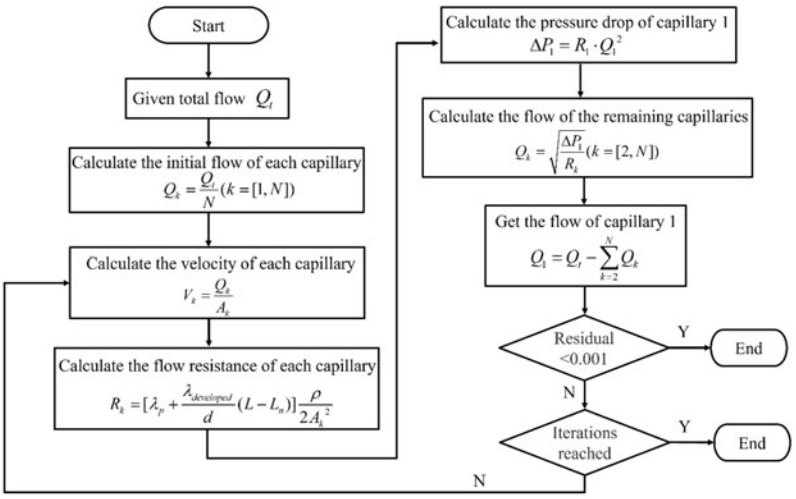

Figure 7. Flow chart of the computational algorithm. Where N represents the number of capillaries and A_k represents the cross-sectional area of each capillary.

Table 2. Inner diameter parameter table of different pressure drop standards.

Sample ID	Capillary no. (mm)									
	d1	d2	d3	d4	d5	d6	d7	d8	d9	d10
1	0.643	0.635	0.634	0.635	0.630	0.630	0.622	0.637	0.640	0.635
2	0.538	0.532	0.543	0.539	0.545	0.548	0.544	0.548	0.536	0.542
3	0.479	0.484	0.485	0.477	0.491	0.486	0.481	0.484	0.478	0.480
4	0.452	0.442	0.480	0.463	0.454	0.458	0.450	0.463	0.445	0.452
5	0.432	0.417	0.429	0.422	0.418	0.417	0.427	0.416	0.413	0.424
6	0.413	0.422	0.412	0.415	0.432	0.428	0.420	0.418	0.414	0.427
7	0.372	0.376	0.376	0.378	0.380	0.389	0.374	0.376	0.400	0.384

as an initial condition for the iteration, the flow rate was set so that it was equally distributed across the capillaries. However, due to slight differences in the diameter and length of each capillary, after one iteration, the flow rate for each capillary would also differ. Therefore, multiple iterations were carried out to obtain more accurate flow rates for each capillary and ultimately to calculate a more precise value of draw resistance. This algorithm was capable of converging to a precise value, primarily due to its explicit optimization objective: the pressure drops of the pressure drop standards. In each iteration, the algorithm updates the flow rate of each capillary to calculate the pressure drop of the pressure drop standard. Moreover, the algorithm's termination condition was set such that when the difference between the pressure drops in two consecutive iterations was less than 0.001, the algorithm ceased to iterate. This termination condition is a typical criterion for convergence. If this condition is met within a finite number of iterations, we could assert that the algorithm had indeed converged.

The program was designed according to the MVVM (Model-View-View model) pattern. The view was responsible for the appearance of the interface of the entire program, the view model was responsible for modeling the content presented in the interface, and the model was also used to store data. The interface was developed using WPF (Windows Presentation Foundation), the latest generation of Microsoft's graphics system, and the logical functions of the program were implemented in C#.

The program allows for the input of experimental environmental parameters (temperature, humidity, atmospheric pressure) and reads the diameter and length of the ten capillaries of the pressure drop standard obtained from OGP testing in a comma-separated values (CSV) format. Following the logic outlined in theoretical analysis, the program performed iterative calculations.

The iteration process was guided by the criterion that the difference in pressure drop between two consecutive steps should be below 10^{-3} Pa or reached the maximum number of iterations, upon which the calculation loop was terminated. Ultimately, the program computed the draw resistance of the pressure drop standard, the flow rate for each capillary, and the proportion of the development length to the total length. The results were then displayed in the interface, providing a comprehensive presentation of the calculations performed.

RESULTS AND DISCUSSION

Experimental testing was conducted on seven different specifications of pressure drop standards using an optical gaging product (OGP). This led to the acquisition of geometric structure data for the draw resistance standard rods. The results are presented in Table 2.

The theoretical pressure drop values under the corresponding environmental conditions were obtained by iterative calculations of the program, and the comparison results are shown in Table 3.

The data presented in Table 3 demonstrate a consistent trend between the experimental and calculated values, with all relative errors falling below 8%. This consistency underscores the reliability of our methods and calculations. However, it is important to note that the pressure drop standard, due to its manufacturing process, does not always exhibit a perfect circular shape in its capillaries. This imperfection is a contributing factor to the observed errors. Despite this, the overall trend remains consistent, reinforcing the validity of our approach. A comparative analysis of the experimental and calculated values is illustrated in Figure 8. This visual representation further elucidates the correlation between these two sets of data, providing a

Table 3. Comparison of experimental and calculated values.

Sample ID	Experimental draw resistance (Pa)	Calculated draw resistance (Pa)	Relative error (%)
1	980.6	974.39	−0.63
2	1972.0	1875.04	−7.10
3	2916.2	2903.03	−0.45
4	3805.2	3634.33	−4.49
5	4825.1	4836.75	0.24
6	5712.2	5377.19	−5.86
7	7971.9	7513.70	−5.75

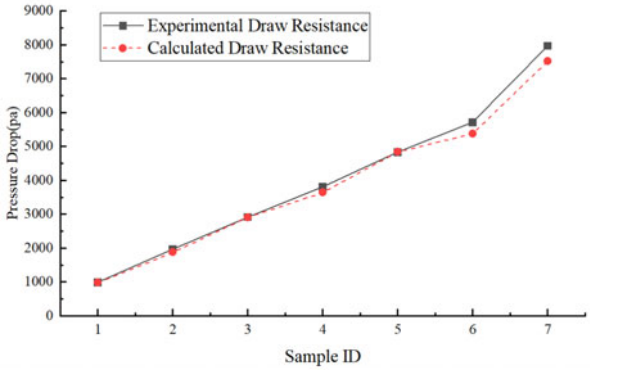

Figure 8. Comparison of experimental and calculated values.

clear and comprehensive overview of our findings.

In the area of commercially available pressure drop standards, the prevailing practice relies on empirical methods for designing the dimensions of the capillaries, followed by their one-time encapsulation using capillary glass tubes and epoxy or acrylic resin. However, this design approach lacks a sound theoretical basis, leading to a relatively low qualification rate of the pressure drop standards. To address this issue, we undertook a research study focusing on pressure drop standards with varying structural parameters, and developed a mathematical model to investigate the internal airflow dynamics within these standards. The mathematical model took into account the distribution characteristics of the internal airflow within the pressure drop standards, encompassing laminar inlet effects and the development and fully developed zones inside the capillary. These factors have the potential to impact the suction resistance values of the pressure drop standards. Existing models, in contrast, may overlook these factors, relying solely on energy loss coefficients to characterize the flow dynamics of pressure drop standards. Consequently, the mathematical model was poised to more accurately depict the internal airflow state of the pressure drop standards, thereby enhancing predictive capabilities. Utilizing this model, we calculated the relationship between the dimensions (diameter and length) of the capillaries in the pressure drop standard and the corresponding flow rate and draw resistance. In order to validate our model, we compared experimentally measured draw resistance values of the pressure drop standards with their corresponding theoretical values. Based on the results presented in Table 3, we observed that, for the seven different pressure drop standards, the model yielded a prediction error that was generally below 8%. These findings provide a solid theoretical foundation for the design and manufacturing of pressure drop standards, thus contributing to their overall improvement.

CONCLUSION

In this paper, the diameter and length of the capillaries in a pressure drop standard were measured by OGP image measuring instrument, and a theoretical model of the gas flow in the pressure drop standard was established based on the flow distribution according to the theory of laminar flow in circular tubes including a turbulent inlet section, and an iterative calculation program was written. The theoretical and experimental differential pressure values of seven pressure drop standards were compared and analyzed. The trends of the theoretical and experimental values did not show significant differences, and the relative errors were below 8%, so the theoretical model can provide support for the design of pressure drop standards.

AUTHOR CONTRIBUTIONS

Conceptualization: P.Z. and C.L.; methodology: P.Z.; software: C.L.; validation: P.Z., C.L. and Z.S.; formal analysis: R.Y.; investigation: Z.C.; resources: Q.M.; data curation: P.Z.; writing-original draft preparation: P.Z. and C.L.; writing-review and editing: Z.C. and K.Z.; visualization: K.Z.; supervision: R.Y.; project administration: Q.M.; funding acquisition: Q.M. All authors have read and agreed to the published version of the manuscript.

FUNDING

This research was funded by development and validation of low pressure drop standards and slim ventilation rate standards, grant number: The standard pre research project of State Tobacco Monopoly Administration, [2021] No. 55.

DATA AVAILABILITY STATEMENT

Not applicable.

CONFLICTS OF INTEREST

The authors declare no conflict of interest.

REFERENCES

1. Miao Q., J. Cheng, H. Zhao, R.C. Yang, and Z.D. Su: The Effects of Pressure and Humidity Variations on Pressure Drop of the Draw Resistance Standard Rod; Appl. Mech. Mater. (2014) 20–23. DOI: 10.4028/www.scientific.net/AMM.543-547.20
2. International Organization for Standardization (ISO): ISO 6565:2015: Tobacco and Tobacco Products – Draw Resistance of Cigarettes and Pressure Drop of Filter Rods – Standard Conditions and Measurement; ISO, Geneva, Switzerland, 2015. Available at: https://www.iso.org/standard/64265.html (accessed June 2024)
3. Yang, R., B. Zeng, H. Zhao, P. Zhang, Z. Shi, Q. Yu, Q. Zhang, D. Li, L. Fan, and Q Miao: Calibration of Pressure Drop Standards Based on Volume Flow (In Chinese); Tob. Sci. Technol. 54 (2021) 96–100. DOI: 10.16135/j.issn1002-0861.2021.0059
4. Fan, L., Q. Miao, H. Zhao, and Q. Zhang: Influence of Atmospheric Pressure on Measurements of Draw

Resistance of Cigarette and Pressure Drop of Filter Rod (in Chinese); Tob. Sci. Technol. (2004) 5–7.
5. Keith,C.H. and A. Corbin: Multiple Capillary Pressure Drop Standards; Beitr. Tabakforsch. 8 (1975) 60–64. DOI: 10.2478/cttr-2013-0356
6. Colard, S., W. Trinkies, G. Cholet, B. Camm, M. Austin, and R. Gualandris: Compensation for the Effects of Ambient Conditions on the Calibration of Multi-Capillary Pressure Drop Standards; Beitr. Tabakforsch. Int. 21 (2004) 167–174. DOI: 10.2478/cttr-2013-0777
7. International Organization for Standardization (ISO): ISO 3402:2023: Tobacco and Tobacco Products – Atmosphere for Conditioning and Testing: ISO, Geneva, Switzerland, 2023. Available at: https://www.iso.org/standard/83089.html (accessed June 2024)
8. Wang, Z.Q.: Study on the Correction Coefficients of Liminar and Turbulent Entrance Region Effect in a Round Tube; App. Math. Mech. 3 (1982) 393–406. Available at: https://www.amm.shu.edu.cn/EN/Y1982/V3/I3/433 (accessed June 2024)
9. Nikuradse, J.: Laws of Flow in Rough Pipes; Technical Memorandum 1292, NACA TM 1292, National Advisory Committee For Astronautics (NACA), Washington, USA, 1950. Available at: https://ntrs.nasa.gov/citations/19930093938 (accessed June 2024)

Corresponding author:

Qian Miao
Zhengzhou Tobacco Research Institute of CNTC
Zhengzhou 450001
China
E-mail: miaoq@ztri.com.cn